

Performance and Analysis of UWB Aesthetic Pattern Textile Antenna for WBAN Applications

T. Annalakshmi¹ and S. Ramesh²

¹Department of Electronics and Communication Engineering
New Prince Shri Bhavani College of Engineering and Technology, Chennai – 600074, Tamil Nadu, India
lakshmishanmu15@gmail.com

²Department of Electronics and Communication Engineering
SRM Valliammai Engineering College, Kattankulathur, Chennai - 603203, Tamil Nadu, India
rameshs.ece@valliammai.co.in

Abstract — This article proposes a new aesthetic pattern-three petal flower patch antenna that operates at Ultra Wide Band (UWB) for Wireless Body Area Network (WBAN) applications. The flower structure consists of three petals and a center circle patch with the partial ground plane at the bottom. A double-sided copper-coated conductive fabric, which is 0.08 mm thick, having a surface resistivity of 0.05 Ω /square, serves as the antenna patch and ground material. This conductive patch is placed in a denim jeans material with 1mm thick that forms the substrate. The utilization of a two-layer substrate and partial ground method enhances the impedance bandwidth of the antenna. The size of the antenna is 60 mm \times 60 mm \times 2.16 mm. The reflection coefficient, gain, efficiency, radiation pattern, and effects of bending were the various parameters analyzed for the flower antenna. The antenna radiates from 3 to 12 GHz, which covers the entire UWB frequency range from 3.1 to 10.6 GHz assigned by Federal Communications Commission (FCC). The measurement results validate the performance of a flower patch antenna.

Index Terms — Aesthetic pattern, laser-cut fabrication, partial ground, thick substrate, UWB, WBAN.

I. INTRODUCTION

The Market revenue of wearable devices is expected to leap at quadruple pace and reach \$150 bn by the year 2026. Smart clothing segment, within wearable devices, have dynamic development, with fitness and fashion collaborating to create unique applications and trends within this segment [1, 2]. Ease in the availability of data, IoT, and acceptance at large wearable devices further boost this segment's growth. Wearable devices need to be of an adept design and created with ease; they need to be in-vogue, be captivating and irresistible and need to deliver the intent. Flexibility and breaking the norm on geometric patterns of the underlying technology

of wearable devices is the way to enable them to be designed and created to be appealing to the masses across age groups and geography. This paper intends to prove that the fabrication of the antenna can be customized and designed to adapt to work in the UWB frequency range. It is most adapted for the fast-developing WBAN applications while retaining technical capabilities and reliability [3, 4].

Several kinds of research have been undertaken on enhancing the bandwidth of antenna for wearable applications. Some of the essential and noteworthy investigations have been cited below for reference: in [5], to cover the ultra-wideband, a Y shaped monopole antenna with the etched inverted bell-shaped slot in the partial ground was proposed. In [6], devoted a wearable antenna operates from 3.2-16.3 GHz. They introduced a Co- Planner Waveguide (CPW) structure with slots on the ground plane to increase bandwidth. In [7, 8], to improve the bandwidth, multiple resonators and slots were used. In [9], a multi-stacked patch is used with CPW feed to increase the bandwidth. In [10], combinations of parasitic patches are used for broadening the frequency range. In [11], the broadband was realized by combining the zeroth-order resonator (ZOR) structure with a micro strip patch. In [12], making edge truncation in the radiator and partial ground plane wideband is achieved. A rectangular slot antenna with reduced ground size and offset feeding is proposed to enhance the bandwidth [13]. A fractal antenna with a partially modified elliptical ground was designed to cover frequency from 1.4 to 20 GHz [14]. In [15], dual-band is achieved by the reactive loading in the form of a shorting pin and two arc-shaped slots introduced in the patch. In [16], to cover the UWB range, a lengthy slot, and the partial ground was used. In [17], the flower-shaped patch antenna designed with CPW feeding to achieve wideband impedance matching. Several kinds of patch and slot antennas were reported for UWB application in recent years [18-20].

Based on these various cited studies and its results, the new aesthetic pattern-three petal flower patch antenna with the partial ground in a thick substrate with low dielectric constant material that operates at UWB has been introduced. It can be used in real-time wearable WBAN applications such as health monitoring, physical training, and navigation. This antenna has been designed using wearable technology to be applied to cloth, which will easily reach the masses. This article consists of four sections. Section II elaborates on the antenna geometry and fabrication method. In Section III, discussed the antenna result and its performance. Section IV presents the conclusion.

II. ANTENNA DESIGN

A. Antenna geometry

Figures 1 (a) and (b) depict the three petals flower textile antenna geometry and side view and simulated using CST Microwave Studio to utilize the finite integration technique. Using a three-point spline curve method, the flower shape antenna is formed, which is available in the CST-microwave studio 16 software.

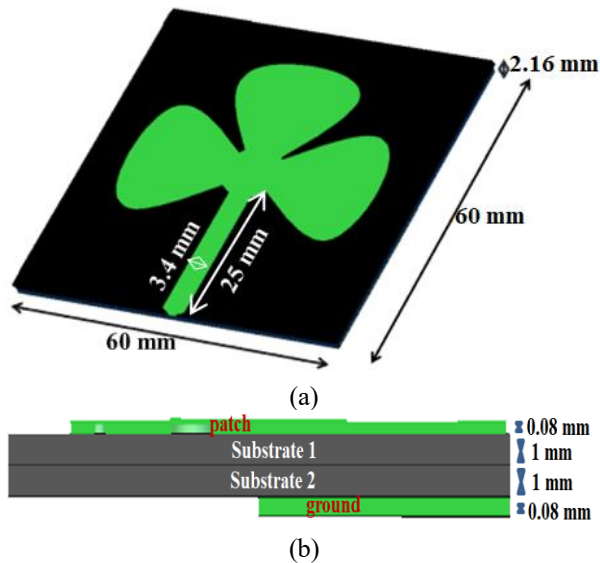


Fig. 1. (a) Antenna geometry and (b) side view of the proposed antenna.

The top layer of the antenna acts as a patch, consisting of three petals, a circle at the center, and a feed line. Table 1 gives the dimension of the flower patch. The X and Y-axis represent the orientation of every petal. The radius of the center circle is 5 mm, and the length and width of the feed line are 25 mm, 3.4 mm, respectively. The patch is made up of double-sided copper conductive fabric. The surface resistivity of the conductive fabric is 0.05 Ω /square. Its base material is polyester and coated with copper and nickel, while the thickness is 0.08 mm.

Table 1: The dimension of petals

	Xmin	Xmax	Ymin	Ymax
	Dimensions in mm			
Petal1	-10.84	10.84	34	52.89
Petal2	-22.89	-4	19.15	40.84
Petal3	4	22.89	19.15	40.84

Table 2: Component of conductive fabric

Component	Composition (%)
Polyester	70 \pm 3
Copper	16 \pm 5
Nickel	14 \pm 2

Table 2 depicts the material basis and content of the conductive fabric. As the microstrip antenna has inherent narrow band characteristics, two methods have been explored to increase the bandwidth. In the first method, there is an increase in the substrate thickness with lower dielectric constant material. Thick substrates with a smaller range of dielectric constant are the most desired as they provide higher bandwidth and efficiency [21]. In general, the dielectric constant of textiles material has low value and reduces the surface wave losses. Here a denim jeans material is used as a substrate with dielectric constant of 1.7, loss tangent of 0.025 with a thickness of 1mm [22]. The thickness of the denim jeans material is measured using a vernier caliper. To increase the thickness, two layers are sandwiched and serve as a thick intermediate substrate. The dimension of the substrate is 60 \times 60 mm. In the second method, there is a reduction in ground size in half of the substrate size for bandwidth improvement. The bottom layer serves as a ground. The dimension of the ground is 60 \times 30 mm in length and width. It is made up of copper coated fabric, which is the same as patch material.

B. Fabrication method

The antenna has been fabricated using flexible copper fabric material and shaped using a laser cutting machine [23]. Laser cutting is suitable for metal, plastic, paper, and fabric. The conductive fabric is cut to appropriate dimensions at the bottom and top layer to make the antenna resonate at the corresponding band using the laser machine SENFNNG –SF1610. A laser cutting machine works by focusing a beam of laser light on a piece of material. The laser light is highly powered when it is focused, and it raises the temperature of the material to be cut high enough to melt it in the small area where the beam is focused. The laser's head is moved using some form of the gantry to position the beam to cut shapes over the material. The laser cutting process uses a contactless beam to generate heat, causing the fabric to melt and vaporize the workspace. The weakening and removal of

the affected area of the material form the desired cut without causing any damages. The advantages of laser cutting are extreme accuracy, clean cuts, and sealed fabric edges to prevent fraying. The precisely cut flower pattern fabric and ground fabric are attached to a denim substrate using fabric glue. This antenna will be produced to custom specification and shipped to the cloth manufacturing unit, where it can be attached to the cloth by simple sewing method.

Front and back view of the fabricated antenna shown in Figs. 2 (a) and (b). A microstrip feed line is used to excite the flower patch using a $50\ \Omega$ SMA connector. In real-time scenarios, the existing microstrip line in the cloth and a flexible co-axial cable connects to the radio equipment, which acts as the transceiver [24]. Simple snaps used across the clothing industry can be used as the connector between the microstrip line and co-axial cable [25]. This will ease the work of the end-user creating a simple fastener to make or break the connection as required. The advantages of the snaps are cheap, easy to fix, and withstand wear and tear due to washing.



Fig. 2. The fabricated antenna: (a) front view and (b) back view

III. RESULT AND DISCUSSIONS

The antenna was exposed to free space and near the human body environment to study the following parameters such as reflection coefficient, radiation pattern, gain, efficiency, and bending performance. The Gustav Voxel model available in the CST software was used for the simulation of an on-body environment [22]. Fig. 3 depicts the picture of on body model where the antenna is placed on the chest.

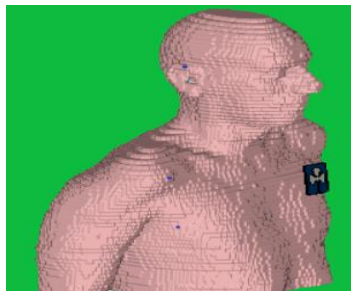


Fig. 3. Antenna placed on the chest of Gustav Voxel model.

A. Reflection coefficient

The measurement of reflection coefficient (S11) obtained using a vector network analyzer (VNA) in the frequency range of 0 to 22 GHz. A connection of VNA to a PC with interfacing software calibrates the S11 in short-open load through (SOLT) standards. Figure 4 shows the reflection coefficient characteristics of the antenna measured on free space and the on-body simulated environment when plotted against free space simulation. In the simulation, the antenna produces the impedance bandwidth of 9 GHz from 3 to 12 GHz frequency range, which covers the entire UWB band. On the other hand, the measured and on-body simulated result shows the same bandwidth with a slight variation in the level of reflection coefficient. The difference between simulation and measurements were observed in the found result. The difference in the reflection coefficient in the free space environment may be due to errors during the fabrication as the prototype is flexible, losses in SMA connector used, and due to the cable losses and connection repeatability with the feeding cable. Similarly, in the on-body simulation, the loss could be due to an on-body structure. The simulation and the measured result show that the antenna fulfills the bandwidth requirement of the UWB band.

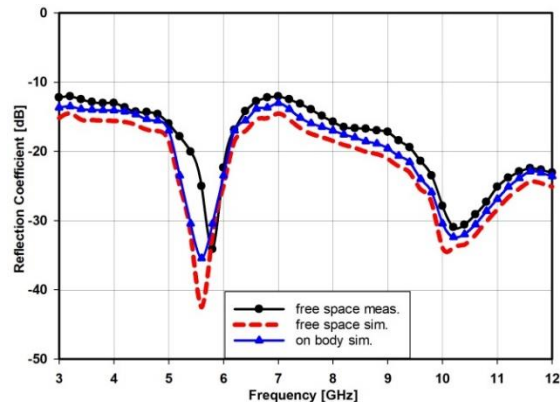


Fig. 4. Reflection coefficient comparison for simulation and measurement values.

B. Gain and efficiency

The gain and efficiency response of the proposed antenna is shown in Fig. 5. From the graph, we observe that the gain varies in the range of $-1.29\ \text{dB}$ (3 GHz) to $2.35\ \text{dB}$ (12 GHz) whereas the measured gain lies in the range of $-2.22\ \text{dB}$ (3 GHz) to $1.35\ \text{dB}$ (12 GHz) over the operating frequency band. In real measurement, antenna gain is calculated using the anechoic chamber. It uses the pyramidal horn as the transmitting antenna, which produces 15 dB gain in the frequency range of 600 MHz to 18 GHz. The proposed antenna acts as a receiver antenna kept with a distance of 5.7 m from the transmitter antenna. Similarly, in the on-body simulation the gain

value varies from -1.79 dB (3 GHz) to 1.8 dB (12 GHz). The gain of the flower antenna measured from the chamber and on-body simulations are in good agreement with free space simulated gain over the entire operating band. Besides, it is observed that the simulated radiation efficiency in free space lies in the range of 0.69 to 0.76 and 0.65 to 0.71 in on-body simulation over the entire operating frequency range.

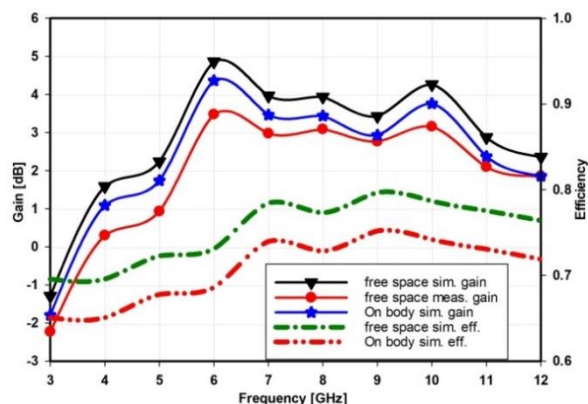


Fig. 5. The gain and efficiency response of the proposed antenna.

C. Radiation pattern

Figure 6 shows the radiation pattern measurement setup in E-plane and H-plane directions using the fully shielded anechoic chamber. The chamber's working frequency ranges from 700 MHz to 18 GHz with a dimension of 5.7 m × 3.5 m × 3 m. The study of the radiation pattern of the proposed antenna in the H plane and E plane directions at 4, 7, and 10 GHz is shown in Figs. 7 (a), (b) and (c). The value of phi is 0° for all theta values to arrive at the radiation pattern in the E plane. Similarly, to attain the H plane's radiation pattern, phi has been set as 90° for all theta's values. In all the specified frequencies, the H-plane pattern shows that the radiation pattern is bidirectional. In E-plane, the radiation is omnidirectional. It is observed that in both planes, there is a proper matching between free space. On-body simulation, and measured patterns in the predetermined frequencies.

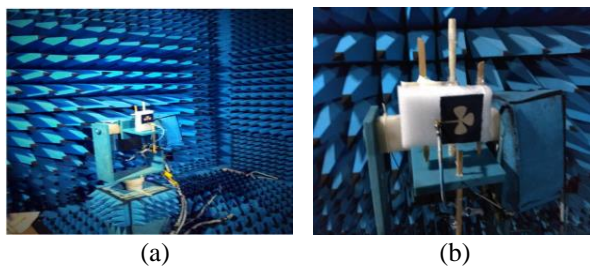


Fig. 6. Radiation pattern setup in chamber: (a) H-plane direction and (b) E-plane direction.

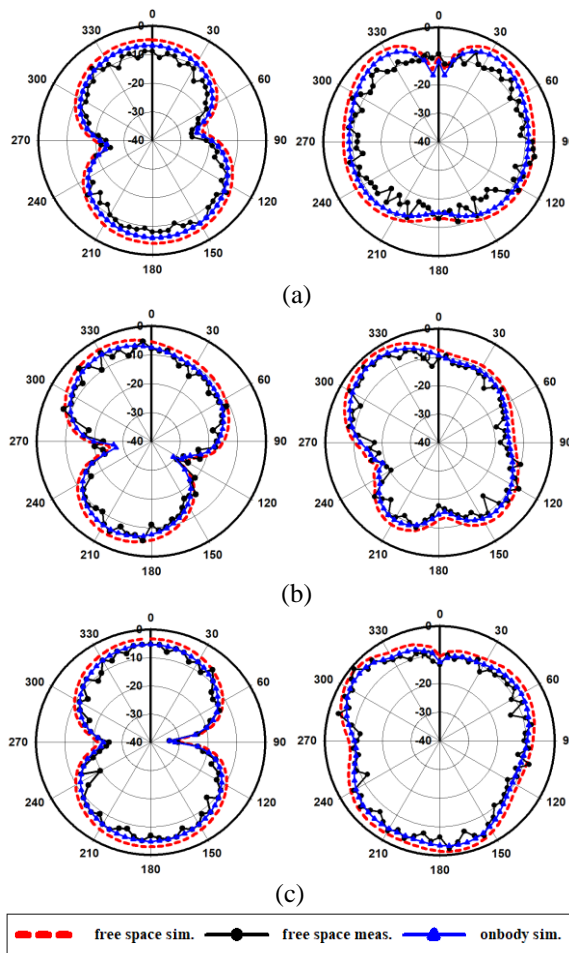


Fig. 7. Simulated and measured radiated pattern in H-plane direction (left) and E-plane direction (right) for: (a) 4 GHz, (b) 7 GHz, and (c) 10 GHz.

D. Bending performance

WBAN applications should have the inherent capacity to retain their technical features even when they are bent, as they expect to align with the body movement of the person who would be wearing them.

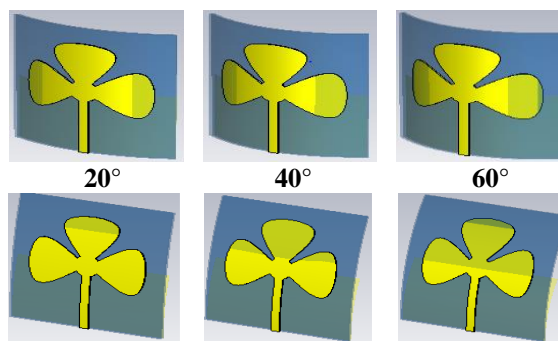


Fig. 8. Antenna bending at E-plane direction (top row), H-plane direction (bottom row) in various angle.

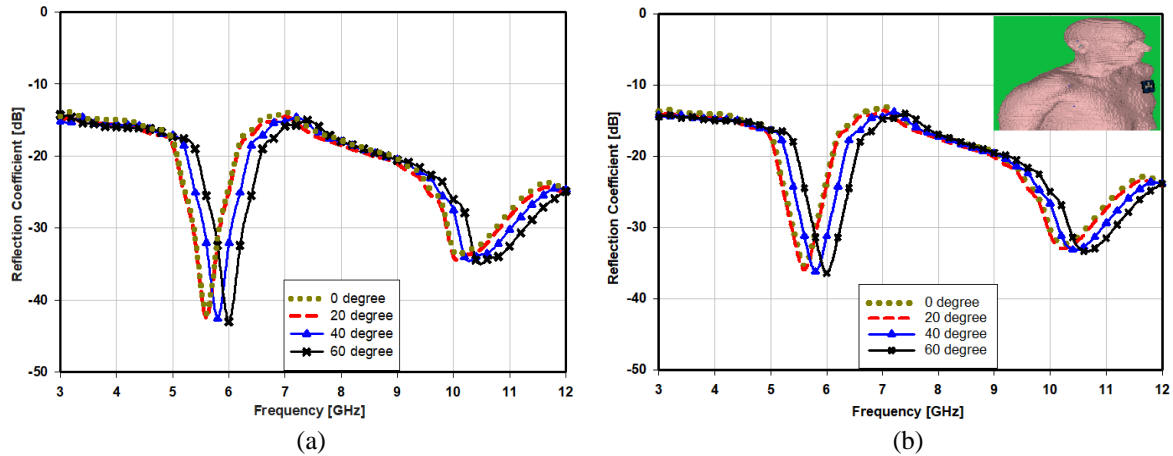


Fig. 9. Bending performance at E-plane direction: (a) free space simulation and (b) on-body simulation.

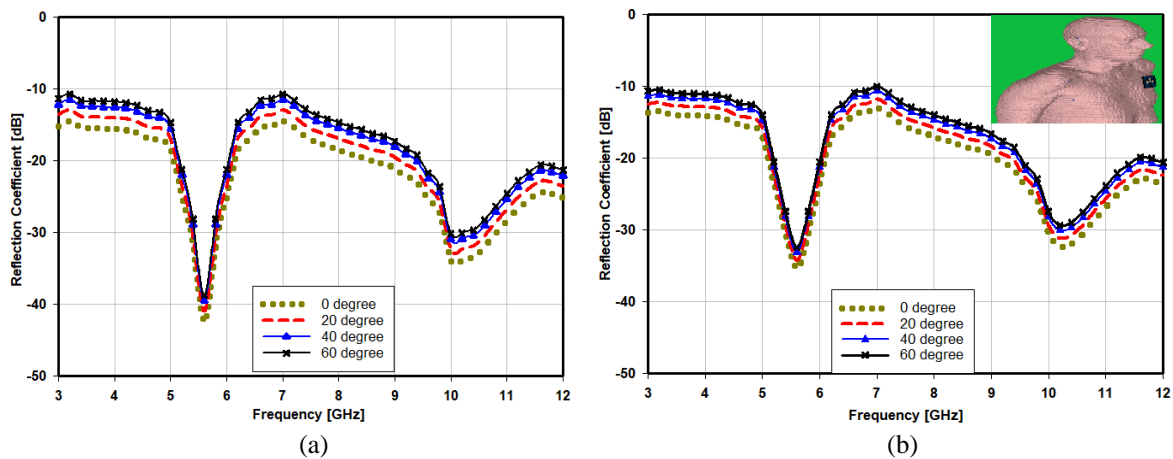


Fig. 10. Bending performance at H-plane direction: (a) free space simulation and (b) on-body simulation.

There were three bending angles considered for the study in E and H-plane direction. Figure 8 shows antenna bending in E-plane and H-plane direction at 20°, 40°, and 60° angles. In Figs. 9 and 10 the simulated reflection coefficient characteristics of the antenna is studied at various angles on both free space and on body simulation environment. The reflection coefficient of flower antenna with different angles was compared with 0° angle (flat antenna) in E-plane and H-plane directions. In both bending directions for 20°, 40°, and 60°, the antenna provides the required bandwidth from 3 to 12 GHz in free space and on-body environment. From the results, we can say that the proposed antenna is working as expected in all bending conditions, and the reflection coefficient was found identical for all angles compared to the flat antenna. Only a small fluctuation was found at a higher bending angle of 60° in both directions due to the impedance transition direction.

E. Surface current

Figure 11 depicts the surface currents of the

proposed flower antenna. The surface current shows the actual electric current that is induced by an applied electromagnetic field. From the figure, we see that the current distribution is equal in all the three petals, the maximum surface current is 31.3 A/m. From the direction of current distribution, we observe that the antenna is vertically polarized.

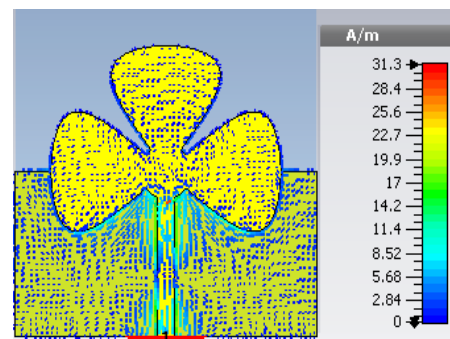


Fig. 11. The surface current of proposed antenna.

IV. CONCLUSION

The Aesthetic pattern patch antenna has been designed to operate at UWB frequency, which supports WBAN application. This antenna has been fabricated with commonly available daily wear jean material as a substrate using a simple fabrication technique, which makes it very cost-effective and robust. The patch and ground are also made using copper fabric. Both materials are very flexible and more comfortable for regular wearable purposes. The attractive flower shape patch inspires the people to wear. The proposed antenna provides sufficient reflection coefficient, gain, and efficiency in the operating band.

Furthermore, it produced excellent radiation characteristics in simulation and measurements. The radiation pattern of the proposed antenna in the H-plane is bidirectional, and in E-plane, it provides an omnidirectional pattern. Also, the antenna works well in E and H-plane bending direction. These features make the antenna aptly suited for real-time wearable WBAN applications such as health monitoring, physical training, and navigation. The application of this antenna can range from simple day to day applications to sophisticated medical devices and military applications with the explosion of IoT.

ACKNOWLEDGMENT

The authors wish to acknowledge DST-FIST supporting facilities in the department of Electronics and Communication Engineering, SRM Valliammai Engineering College, Chennai, Tamil Nadu, India.

REFERENCES

- [1] J. Tak and J. Choi, "An all textile Louis Vuitton logo antenna," *IEEE Antennas and Wireless Propagation Letters*, vol. 14, pp. 1211-1214, 2015.
- [2] G. W. Whittow and M. J. Rigelsford, "Performance and radiation patterns of aesthetic and asymmetric logo-based patch antennas," *Journal of Electromagnetic Waves and Applications*, vol. 28, pp. 848-860, 2014.
- [3] A. Mersani, L. Osmman, and I.-M. Ribero, "Flexible UWB AMC antenna for early stage skin cancer identification," *Progress in Electromagnetics Research*, vol. 80, pp. 71-81, 2019.
- [4] R. Bala, R. Singh, A. Marwaha, and S. Marwaha, "Wearable graphene based curved patch antenna for medical telemetry applications," *ACES Journal*, vol. 31, no. 5, pp. 543-550, May 2016.
- [5] P. Sambandam, M. Kanagasabai, S. Ramadoss, R. Natarajan, M. G. N. Alsath, S. Shanmuganathan, M. Sindhadevi, and S. K. Palaniswamy, "Compact monopole antenna backed with fork slotted EBG for wearable applications," *IEEE Antennas and Wireless Propagation Letters*, vol. 19, pp. 228-232, 2020.
- [6] S. M. H. Varkiani and M. Afsahi, "Compact and ultra-wideband CPW-fed square slot antenna for wearable applications," *AEÜ International Journal of Electronics and Communications*, vol. 106, pp. 108-115, 2019.
- [7] B. V. B. R. Simorangkir, A. Kiourti, and P. K. Esselle, "UWB wearable antenna with full ground plane based on PDMS embedded conductive fabric," *IEEE Antennas and Wireless Propagation Letters*, vol. 17, pp. 493-496, 2018.
- [8] W. Yao, H. Yang, X. Huang, and Z. Yu, "A four-leaf clover shape MIMO antenna for UWB applications," *ACES Journal*, vol. 31, no. 12, pp. 1421-1425, Dec. 2016.
- [9] A. L. Y. Poffelie, P. J. Soh, S. Yan, and A. E. G. Vandenbosch, "A high fidelity all-textile UWB antenna with low back radiation for off-body WBAN applications," *IEEE Transactions on Antennas and Propagation*, vol. 64, no. 2, pp. 757-760, 2016.
- [10] B. P. Samal, P. J. Soh, and A. E. G. Vandenbosch, "UWB all-textile antenna with full ground plane for off-body WBAN communications," *IEEE Transactions on Antennas and Propagation*, vol. 62, no. 1, pp. 102-107, 2014.
- [11] K. Sun, L. Peng, Q. Li, X. Li, and X. Jiang, "Compact Zeroth-order resonance loaded microstrip antenna with enhanced bandwidth for wireless body area networks/brain activity detection," *ACES Journal*, vol. 33, no. 6, pp. 631-640, June 2018.
- [12] S. Mohandoss, S. K. Palaniswamy, R. R. Thipparaju, M. Kanagasabai, B. R. B. Naga, and S. Kumar, "On the bending and time domain analysis of compact wideband flexible monopole antennas," *AEÜ International Journal of Electronics and Communications*, vol. 101, pp. 168-181, 2019.
- [13] K. Shafique, A. B. Khawaja, A. M. Tarar, M. B. Khan, M. Mustaqim, and A. Raza, "A wearable ultra-wideband antenna for wireless body area networks," *Microwave and Optical Technology Letters*, vol. 58, no. 7, pp. 1710-1715, 2016.
- [14] M. Karimyian-Mohammadabadi, M. A. Dorostkar, F. Shokuohi, M. Shanbeh, and A. Torkan, "Super-wideband textile fractal antenna for wireless body area networks," *Journal of Electromagnetic Waves and Applications*, vol. 29, no. 13, pp. 1728-1740, 2015.
- [15] B. V. B. R. Simorangkir, Y. Yang, L. Matekovits, and P. K. Esselle, "Dual-band dual-mode textile antenna on PDMS substrate for body-centric communications," *IEEE Antennas and Wireless Propagation Letters*, vol. 16, pp. 677-680, 2016.
- [16] N. Chahat, M. Zhadobov, R. Sauleau, and K. Ito, "A compact UWB antenna for on-body

- applications,” *IEEE Transactions on Antennas and Propagation*, vol. 59, no. 4, pp. 1123-1131, Apr. 2011.
- [17] S. R. Patre and P. S. Singh, “CPW-fed flower-shaped patch antenna for broadband applications,” *Microwave and Optical Technology Letters*, vol. 57, no. 12, pp. 2908-2913, 2015.
- [18] M. NejatiJahromi, M. N. Jahromi, and M. Rahman, “A new compact planar antenna for switching between UWB, narrow band and UWB with tunable-notch behaviors for UWB and WLAN applications,” *ACES Journal*, vol. 33, no. 4, pp. 400-406, Apr. 2018.
- [19] Z.-L. Song, Z.-J. Zhu, and L. Cao, “High isolation UWB-MIMO compact micro-strip antenna,” *ACES Journal*, vol. 33, no. 3, pp. 293-297, Mar. 2018.
- [20] S. Ramesh and J. Jayalakshmi, “Compact fractal wearable antenna for wireless body area communication,” *Telecommunication and Radio Engineering*, vol. 79, no. 1, pp. 71-80, 2020.
- [21] A. C. Balanis, *Antenna Theory, Analysis and Design*. John Wiley and Sons Inc., New York, 1997.
- [22] I. Gil and R. Fernández-García, “Wearable PIFA antenna implemented on jean substrate for wireless body area network,” *Journal of Electromagnetic Waves and Applications*, vol. 31, pp. 1194-1204, 2017.
- [23] N. Chahat, M. Zhadobov, S. A. Muhammad, L. L. Coq, and R. Sauleau, “60-GHz textile antenna array for body-centric communications,” *IEEE Transactions on Antennas and Propagation*, vol. 61, no. 4, pp. 1816-1824, Apr. 2013.
- [24] A. Sabban, “Active compact wearable body area networks for wireless communication, medical and IoT applications,” *Applied System Innovation*, vol. 1, no. 46, 2018.
- [25] T. Kellomaki, “Snaps to connect coaxial and microstrip lines in wearable systems,” *International Journal of Antenna and Propagation*, vol. 2012, 10 pages, 2012.



T. Annalakshmi received her B. Tech. in Electronics and Communication Engineering from Pondicherry University in the year of 2002, M.E. in Communication Systems from Anna University in the year of 2011, and currently pursuing her Ph.D. in the Department of Electronics and Communication Engineering, SRM Valliammai Engineering College, Chennai. Her research interest includes Antennas & Propagation and Wireless Communications. She is currently working as an Associate Professor in the Department of Electronics and Communication Engineering, New Prince Shri Bhavani College of Engineering and Technology, Chennai with 13 years of experience. She is life time member in ISTE and ISRD.



S. Ramesh received his B.E. in Electronics and Communication Engineering from University of Madras, M.Tech. in Communication Engineering from VIT University, Vellore and received his Ph.D. degree on from SRM University, Chennai, in 2001, 2004 & 2015 respectively. He is currently working as an Associate Professor in the Department of Electronics and Communication Engineering, SRM Valliammai Engineering College, Chennai with experience of 16 years. He is a senior member (S'10-M'17-SM'18) of IEEE Antennas & Propagation Society, Life member in IETE, ISTE, SEMCE, BES. He authored papers in reputed journals and international/national conferences. His area of interest includes Antennas & Propagation and Wireless Communications. He is guiding research scholars in the field of antennas & RF Filter under Anna University, Chennai. He is associated with IEEE AP-S Madras chapter as a member in executive committee during 2018-2019 and IEEE MTT-S Madras Chapter for the year 2017.